NOTATION

x_1, x_2, and x_3 are the orthogonal Cartesian coordinates; v_1, v_2, v_3, dimensional components of the velocity vector; d, thickness of the film; V_0, amplitude of the velocity of wall oscillations; $x = x_1/d$, $y = x_2/d$, $z = x_3/d$, dimensionless Cartesian coordinates; $u_0 = v_1/V_0$, dimensionless velocity of unperturbed flow; p_d, dimensional pressure in the liquid; p_{atm}, gas pressure at the free surface; $p_\alpha = p_{atm}/\rho V_0^2$, dimensionless pressure of gas at the free surface; ρ, density; ν, kinematic viscosity; τ, time; $t = \tau V_0/d$, dimensionless time; ω_*, frequency of oscillations of the wall; $\omega = \omega_* d/V_0$, dimensionless frequency; and $\hat{u}$, $\hat{v}$, p, components of the velocity vector and pressure in the perturbed flow.

LITERATURE CITED

1. E. G. Vorontsov and Yu. M. Tananaiko, Heat Exchange in Liquid Films [in Russian], Tekhnika, Kiev (1972).
2. Yih Chia-shun, "Stability of liquid flowing down an inclined plane," Phys. Fluids, 6, No. 3 (1963).
3. Yih Chia-shun, "Instability of unsteady flow or configurations. Part 1. Instability of a horizontal layer on an oscillating plane," J. Fluid Mech., 31, 737 (1968).
4. S. V. Alekseenko, V. E. Nakoryakov, and B. G. Polusaev, "Waves on the surface of a liquid film flowing vertically downwards," Institute of Thermal Physics, Novosibirsk, Preprint No. 39-79 (1979).

NUMERICAL MODELING OF AN EXPLOSION PLASMA GENERATOR, TAKING INTO ACCOUNT RADIATIVE ENERGY TRANSPORT AND EVAPORATION OF THE WALLS

G. S. Romanov and V. V. Urban

UDC 533.6.011.8:535.2

Using a generalized theoretical model, we study the effect of geometrical dimensions and a variety of physical processes on the operation of the explosion plasma generator.

The present work is a continuation of the theoretical study [1, 2] of the explosion plasma generator developed by A. E. Voitenko (Fig. 1). The principles of operation of this device were discussed in sufficient detail in [1-4]. This makes it possible to turn to the formulation of the problem of numerical modeling of the explosion plasma generator.

In the course of operation of the generator, a detonation wave, by passing over the explosives, accelerates a metal plate up to the velocity 5-6 km/sec [2-4]. The phase velocity of the point on the line of contact of the plate and segment will increase (since $U_\phi = V/\sin\varphi$) as the plate approaches the exit aperature and, from some moment of time, it will exceed the speed of sound c_0 in the metal plate and in the spherical segment. Therefore, the perturbations from the contact line (metal deformations, the melt from the walls, etc.) will not propagate upwards along the flow, and affect the motion of the plate and of the gas. It is probable that this can explain the experimental facts that the plate remains flat during the motion inside the segment (this is seen on the x-ray pulsed picture shown in [5]). Under the action of the detonation wave, shock waves propagate and are reflected from the surface of the plate, and cause its expansion and compression. However, the amplitude of these oscillations is small (it is smaller than the proper thickness of the plate), and is much smaller than the path length of the plate inside the segment. It is known [6] that a compressible plate gains velocity discontinuously, and on incompressible plate gains velocity in a smooth fashion. However, the difference of instantaneous velocities of motion is in

V. I. Lenin Scientific-Research Institute of Applied Physical Problems, Belorussian State University, Minsk.

Translated from Inzhenerno-Fizicheskii Zhurnal, Vol. 43, No. 6, pp. 1012-1020, December, 1982. Original article submitted March 9, 1982.

0022-0841/82/4306-1418$07.50

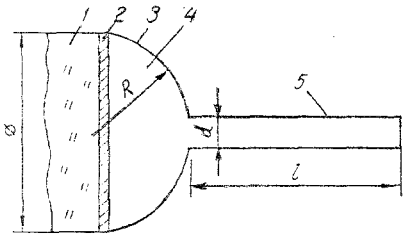

Fig. 1. Diagram of the Voitenko explosion plasma generator: 1) charge of explosives (compressor); 2) plate; 3) working chamber (spherical segment); 4) working gas; 5) exit tube.

both cases relatively large only at the very beginning of the acceleration stage [6]. On the whole, the velocity profile of the compressible plate is a line which oscillates around the smooth curve which represents the trajectory of the incompressible plate. In both cases, the kinetic energies of the plates are almost identical. One can therefore assume that the plate is incompressible and nondeformable, i.e., planar.

The propagation of the detonation wave is determined by the conservation of momentum and mass, and is independent of the specific structure of its front [6]. One can therefore assume the model of instantaneous detonation and neglect in the calculations the narrow region of chemical reaction as was assumed, e.g., in [7]. The system of equations which describe the detonation of explosives, acceleration of the plate, and the gasdynamic flow in the compressor, taking into account the radiative transfer, can be written as follows:

$$\frac{\partial \rho}{\partial t} + \operatorname{div}(\rho \mathbf{w}) = 0, \quad \frac{\partial \rho u}{\partial t} + \operatorname{div}(\rho u \mathbf{w}) + \frac{\partial p}{\partial z} = 0,$$

$$\frac{\partial \rho v}{\partial t} + \operatorname{div}(\rho v \mathbf{w}) + \frac{\partial p}{\partial r} = 0, \quad \frac{\partial \rho E}{\partial t} + \operatorname{div}(\rho \mathbf{w} E + p\mathbf{w} + \mathbf{F}) = Q, \tag{1}$$

$$M \frac{dV}{dt} = \Delta p S. \tag{2}$$

The above condition $u_{ph} > c_0$ makes it possible to neglect the lateral dispersion of the detonation products of a cylindrical charge of explosives. In the calculations one can also ignore the behavior of the parts of the plate and segment which are behind the line of their contact, and can be sheared off during the motion of the plate in the direction of the apex of the segment. Thus, the pressure inside the working chamber of the plate will, in the calculation of the acceleration, be put equal to its average value:

$$p_{cp} = \frac{2\pi}{S} \int_0^r pr\,dr.$$

This makes it possible to simplify the calculations without violating the law of conservation of momentum.

The energy density flux of the proper plasma radiation at the compressor F will be determined from the solution [8] of the spectral quasisteady-state transport equation written for a unidirectional flux along a particular direction τ:

$$\frac{dF_\nu}{d\tau} \varkappa_\nu (B_\nu - F_\nu), \tag{3}$$

where

$$B_\nu = \frac{15}{\pi^4} \frac{\sigma \nu^3}{\exp(\nu/kT - 1)}, \quad \int_0^\infty B_\nu d\nu = \sigma T^4.$$

Estimates of the plasma parameters in the compressor [1-4] show that the generated light fluxes can cause the evaporation of metal surfaces. The material of the wall can be heated up to temperatures higher than critical, and the evaporated substance can be completely car-

ried away by the high-velocity plasma flow along the inner surfaces of the compressor. In these conditions we shall use an approximate method for calculation of evaporation which is based on the assumption of complete absorption of the incident influx by the material of the compressor wall. Disregarding the temperature distribution inside the evaporated medium, we shall write the energy balance on its surface in the following form:

$$F = \lambda J_m + J_\varepsilon. \tag{4}$$

The densities of mass and energy fluxes can be determined from the equations of continuity and energy conservation [9]:

$$J_m = \rho_0 u_p,\ J_e = \varepsilon_0 J_m,\ u_n = \sqrt{kT_0/(2\pi m)},\ \varepsilon_0 = 2kT_0/m + \lambda, \tag{5}$$

$$\rho_0 = \left(\frac{2\pi m v_*^2}{kT_0}\right)^{3/2} \exp\left(-\frac{\lambda m}{kT_0} - 1\right). \tag{6}$$

For $T_0 \sim T_{cr}$ Eq. (6) is no longer valid. Therefore, for $T_0 \geqslant T_* = 2\pi m v_*^2/(3k)$ (T_* is the inflection point of the function ρ_0) the variation of ρ_0 is assumed linear and, accordingly, ρ_0 increases slowly, and for $T_0 \sim 10^2$ eV, it reaches the density of the condensed substance. The point T_* is chosen as a dividing boundary since, according to Eq. (6), below T_* the density increases with temperature, and above T_* it decreases (which is not physically meaningful). In the conditions considered here $T_0 \sim T_{cr}$, there is no model of the state of the substance which is well justified. We shall therefore use interpolations between states with low and high densities of vapor. In particular, the specific internal energy of vapor $T_0 \geqslant T_*$ will be determined by using the approximation of the quantum-statistical model of the atom from tables [10].

We note that this model for the evaporation processes is, in principle, analogous to a model developed in [11], and is based on the assumption of complete absorption of heat flux, and on the condition that the evaporation process is in steady state. Indeed, it can be shown in our case that the latter condition is satisfied. The characteristic time for reaching the steady-state evaporation process can be estimated as follows: $t_y \sim x_0/v$, where $v \sim F\rho\lambda$, $x_0 \sim a/v$. Then $t_y \sim a(\rho\lambda/F)^2$, and for Al ($a = 0,87$ cm^2/c; $\lambda = 11.5$ kJ/g; $\rho = 2.7$ g/cm^3, $t_y \sim 5.4\cdot 10^2\ F^{-2}$. In the working chamber of the generator for $T \sim 10^5$°K [1-4], the energy density of the radiation flux F can reach 10^2-10^3 MW/cm^2, and consequently $t_y \sim 10^{-7}$-10^{-11}. This time is at least an order of magnitude smaller than the characteristic exposure time t_0 of the surfaces of the plate and of the spherical segment. The quantity t_0 can be estimated if one knows the "lifetime" of the part of the generating line of the segment near its point of contact with the plate, which, according to [1, 2], is in contact with the hottest part of the plasma. This time is clearly determined by the phase velocity of the contact point, which, for curvature radius of the spherical segment 4-10 cm and velocity of motion of the plate V ~ 5-6 km/sec, is of the order of 10-100 km/sec. It is known from [1, 2] that the volume of plasma packets is small and has a characteristic dimension of approximately 1 cm. Then $t_0 \sim 10^{-6}$-10^{-7} sec. Consequently, the evaporation process in the compressor can be assumed to be a steady-state one.

The Boundary Conditions. On the left, the detonation products are scattered into vacuum ($p = 0$), and on the right, the flow is determined by the motion of the accelerating plate given by Eq. (2) (Fig. 1). It is assumed that on the symmetry axis and on the stationary solid walls the flow vanishes, i.e., the normal component of the velocity vector is zero: $w_n = 0$. Inside the compressor on the boundary of the plate with gas we have the condition of equality of the velocities $w_n = u = V$.

The boundary condition for the energy density of the radiation flux is that this quantity is zero ($F = 0$) in the direction from the walls towards the gas, and when passing through the symmetry axis.

Thermodynamic and Optical Properties. The system of equations which describes the operation of the explosion plasma generator can be closed by specifying the relations which determine the thermodynamic and optical properties of detonation products, working gas and vapor. For the detonation products, we use an analytical interpolation equation of state [12] which makes it possible to take into account individual properties of several types of explosives (hexogen, tetryl, TG, etc.). The equations of state of air and Xe, calculated by using the system of Sach equations and the approximation of weak nonideality according to Debye and Huckel, were taken from the tables [13] and from the data obtained in [14]. In the calculations these equations were used in the form of tables which were linearly extrapolated to the

TABLE 1. Calculated Variants of the Generators (⌀ = 9.6 cm, d = 1 cm)

No. of variant	R, cm	Working gas	Initial pressure in compressor, atm	Plate stop	Includes radiation and evaporation of walls
1	8	Air	1	Yes	Yes
2	5	»	1	No	»
3	8	»	1	»	No
4	5	Xe	1	Yes	Yes
5	8	»	1	»	»
6	5	»	1	»	No
7	8	»	1	»	»
8	5	Air	11.5	»	Yes
9	5	»	25	»	»

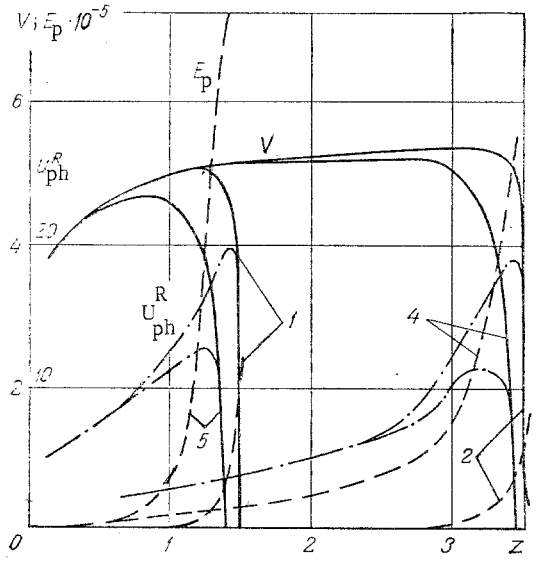

Fig. 2

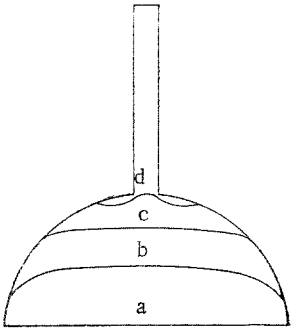

Fig. 3

Fig. 2. The dependence of the velocity of motion of the plate V (solid lines), the radial component of the phase velocity of the point of contact of the plate and segment u^R_{ph} (dash-dot lines), and of the total plasma energy E_p (dashed lines) on the position of the plate in the working chamber. The numbers refer to the numbers of variants in Table 1. V, km/sec; E_p, J; u^R_{ph}, km/sec; z, cm.

Fig. 3. Qualitative pattern of the possible changes of the shape of the plate during its motion in the working chamber.

high temperatures (∿50 eV) and pressures (∿10^7 atm). The error of this extrapolation is small and less than 3 eV in this region. This can be seen from the comparison of the tabulated values used here with the data calculated by using the quantum-statistical model of the atom [15].

The spectral character of the radiation was taken into account in the calculations by using the approximation of three spectral groups, inside which the absorption coefficient was assumed independent of frequency and equal to the spectral absorption coefficient averaged according to Planck. For air, the spectral coefficients were taken from the tables [16] which were extended to the high-temperature region and high energies of quanta. The tables take into account the sharp changes of absorption due to photoionization. For Xe, we used the results of calculations carried out according to the method of [14], which take into account photoionization from the optical and inner shells, free-to-free transitions in the field of ions and neutrals, and the bound-to-bound transitions.

Results of Calculations. To determine the effect of the radius of curvature of the spherical segment, the mass, the thermophysical properties of the working gas, and the role of the radiative transfer and evaporation, we carried out calculations of a number of variants of the explosion plasma generator (see Table 1), which consisted of RDX charge of length 5 cm, mass about 600 g, and total energy 3.5 MJ, and aluminum plates and spherical segments of diameters 9.6 cm, 10, and 16 cm, respectively. The initial mass of the plate was 44 g.

It is seen from Fig. 2 that after the detonation wave reaches the surface of the plate, the plate is accelerated to 4 km/sec over a distance of 2 mm (in a time close to 3 msec). In a variant of the calculation shown in Table 1, the velocity increase of the plate is practically identical. This can be explained by the fact that the effect of the back pressure of the gas is small at this stage. The phase velocity of each point on the line of contact of the plate and segment, in particular, its radial component $u_{ph}^{R} = rV/(R^2-r^2)^{1/2}$, reaches 10-20 km/sec (Fig. 2), and, subsequently, it sharply decreases as a result of the plate being slowed down by the pressure of the plasma and by the decreasing mass of the plate. The deceleration of the plate before reaching the tube, and the character of variation of u_{ph}^{R}, make it possible to describe the qualitative form of the possible deformations of the plate inside the working chamber. If, at the beginning of motion of the plate, the phase velocity is small, e.g., in chambers whose shape is close to semispherical, the plate can be distorted partially by perturbations which propagate from the line of contact with the segment, and also as a result of the decrease of pressure from the center toward the edge during the scatter of the detonation products (Fig. 3b). It is probable that in some variants of the generator this stage of motion of the plate can be accompanied by the propagation of the melt and fragments of the chamber walls and plate, which was observed in the experiment [17]. As the curvature of the surface of the plate increases, the angle of contact and the phase velocity sufficiently decrease so that the propagation of deformations is slowed down. As the plate moves towards the top of the spherical segment, the plate can again become planar as the deformed parts are cut off (Fig. 3c). We note that in the theoretical model the distortions of the shape of the plate can be neglected, since the total energy of the plasma is relatively small at this stage. The plate transfers most of the energy of plasma near the maximum of the phase velocity, when the plate is not yet deformed (Fig. 2). When the plate is decelerated, the plasma energy no longer increases, and the phase velocity becomes smaller than the velocity of propagation of the perturbations in the metal. It is highly probable that in this situation a part of the plasma collapses in a narrow ring-shaped nozzle which is formed by the walls of the plate and of the working chamber. This is so because the plate can bend inside the tube (Fig. 3d), where, according to the calculations, the pressure is lower. In this case only a part of the total quantity of plasma reaches the tube, which, clearly, lowers the potential efficiency of the generator.

In the theoretical model of the explosion plasma generator, we neglected the deformations of the metal walls of the compressor. However, the above assumptions make it possible to analyze the effect of the dimensions of the working chamber of the generator on its operation. Calculations show that, as the radius of curvature of the spherical segment increases, higher pressures and temperatures are reached in the plasma since the phase velocity increases (see Fig. 2). Simultaneously, the increase of the plasma parameters leads to a higher resistance to the motion of the plate, which leads to earlier deceleration and, consequently, to the deformation and increased losses. It is therefore clear that there exists some values of the radii of the segment, which were established experimentally in [3, 4], for which one obtains the maximum parameters of the plasma.

Considerable differences in the operation of the generator are observed when the generator is filled with air and xenon. In the latter case, the total energy of plasma is higher by a factor of 3-4 (see Fig. 2). However, the plate is decelerated to stop considerably earlier, and the energy losses can therefore be considerably higher.

The calculated values of the energetic efficiency (the ratio of the total plasma energy to the energy of the charge of explosives) are as follows: No. 1 — 7.7%, No. 4 — 16.1%, and No. 5 — 21.6% (here and below, the number of the variants corresponds to the number in the table). In the air variants Nos. 2 and 3 (without evaporation), the efficiency was 4.9 and 3.4%, and these quantities are in agreement with the experimental measurements [18]. In the first three above variants, the plate comes to rest, and in the last two variants it passes into the tube. Therefore, the existence of experimental and calculated efficiencies which do not exceed some magnitude $\leqslant$5.7% [18] indicates indirectly the possibility of plasma losses as a result of the plate coming to rest.

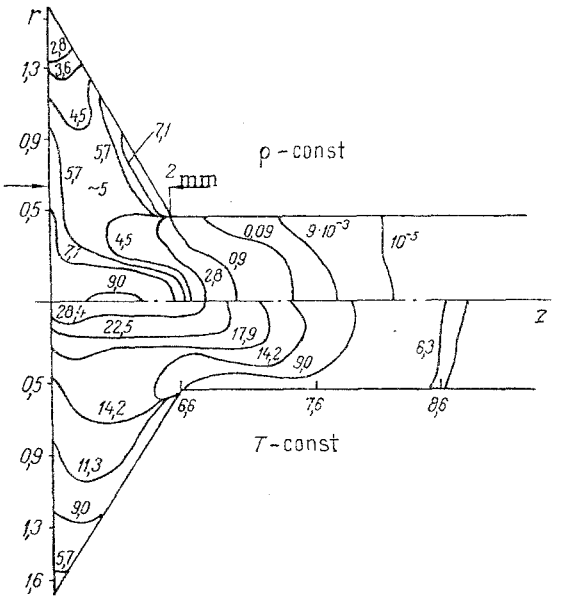

Fig. 4. Spatial flow pattern inside the working chamber and the exit tube for variant No. 5 at the moment that the plate stops. The full lines show the lines of constant density (in g/cm^3; upper half of the figure) and temperature (in eV; lower half of the figure). r, z, cm.

The radiative energy incident on the walls of the working chamber and plate are No. 2 — 2.33 kJ, No. 1 — 10.4 kJ, No. 4 — 23.9 kJ, No. 5 — 63.5 kJ or 1.4-8.7% of the total energy of the plasma. The large irradiation in the xenon variants is due to higher temperatures of the plasma. When the compressor was filled with air at higher pressure (11.5 and 25 atm, Nos. 8 and 9) the fraction of radiation emitted on the wall decreased to 0.3 and 0.16 kJ (0.06 and 0.02% of the total energy of plasma, respectively). This is due to an increased optical thickness of the gas, which depends in the present case on the initial parameters and the subsequent compression of gas by shock waves. In the stage of developed gasdynamic flow when the reflected and lateral waves are present inside the compressor (see [1, 2]), the maximum values of the energy flux density of the radiation in the plasma are reached behind the lateral wave and are 10^2-10^3 MW/cm^2. At the moment of collision of the radial plasma flows formed behind the front of the lateral waves which have velocities close to the maximum phase velocities, a packet with the limiting gasdynamic values reached in the generator is formed at the symmetry axis: $p \sim 10^7$ atm, $\rho \sim 10$ g/cm^3, $T \sim 20$-30 eV.

The initial mass of the working gas can increase by a factor of 1.3-9 because of the vapor of compressor walls. The larger the energy incident on the walls, the larger is the evaporated mass No. 2 — 0.1 g, No. 1 — 0.38 g, No. 4 — 1.56 g, No. 5 — 3.15 g, which is 33.1-87.5% of the total mass of the plasma obtained in the generator before the plate comes to rest or before it passes into the tube. Intense evaporation (e.g., No. 5) can change the pattern of gasdynamic flow in the working chamber, since it leads to the formation of a denser layer of cold vapor near the compressor surfaces (Fig. 4).

The total mass of the plasma has a considerable effect on the operation of the explosion plasma generator, as it causes a premature stopping of the plate in a number of cases. In variants Nos. 8, 9, the main role is played by the initial mass of the gas (2.4 and 5.2 g), since the quantity of vapor is negligible (1.07 and 0.27 % of the total mass of plasma, respectively). In the air variant No. 1, the stopping of the plate is due solely to the influx of vapor, since in calculation without interpolation (No. 3) the plate passes outside the tube, and because it has velocity higher than 2 km/sec, it does not completely transfer its energy to the plasma (the total plasma energy in this case decreases from 260 to 116 kJ). In variants with xenon, one observes both factors (the initial large mass of the working gas, and the large quantity of vapor) and the plate therefore comes to rest (albeit closer to the tube) in the calculations of these variants without evaporation (Nos. 6, 7).

Therefore, an analysis of the obtained results shows that the geometrical and physical parameters of the explosion plasma generator are interdependent, and determine a very distinct individuality of each variant of this device. In conclusion, we shall note that the calculations of the generator were carried out according to the method [1], modified to take into account the detonation process, radiative transfer, evaporation, etc., on lattices 103 × 96 and 82 × 75 in the working chamber and 8 × 120 in the tube. The computation time of this variant, taking into account radiation and evaporation, from the beginning of detonation to the stop of the plate, was 80-90 min on the computer BESM-6.

NOTATION

u_{ph} is the phase velocity; V, velocity of the plate; φ, angle of contact of the plate and spherical segment; c_0, speed of sound in the metal; ρ, density; p, pressure; E, total specific energy; w, velocity; u and v, axial and radial velocity components; F_ν, flux density of radiant energy flux; M, mass of the plate; S, area of the plate; Q, source responsible for the energy dissipation at the detonation front; Δp, difference of pressures to the left and to the right of the plate; r, z, radial and axial coordinates, respectively; t, time; T, temperature; ν, frequency of light; λ, specific heat of evaporation; J_m, flux density of the mass of vapor; J_e, flux density of the energy of vapor; m, mass of an atom of the vapor substance; ν_*, characteristic Debye frequency of the crystal lattice; T_{cr}, critical temperature of the metal; $\varkappa_\nu$, spectral absorption coefficient; $\sigma = 1.0302 \cdot 10^3$ MW/eV^4/m^2, Stefan–Boltzmann constant; and $k = 1.38 \cdot 10^{-23}$ J/°K, Boltzmann constant. The index ν refers to the spectral dependence of the quantities, and 0 refers to the metal walls.

LITERATURE CITED

1. G. S. Romanov and V. V. Urban, "Numerical modeling of an explosion plasma generator in the gasdynamic approximation," Inzh. Fiz. Zh., 37, 859 (1979).
2. G. S. Romanov and V. V. Urban, in: Dynamics of Continuous Medium. Nonstationary Problems of Hydrodynamics. [in Russian], Institute of Hydrodynamics, Siberian Branch, Academy of Sciences of the USSR, No. 48 (1980), pp. 121-129.
3. A. E. Voitenko, "Generation of large-velocity gas jets," Dokl. Akad. Nauk SSSR, 158, No. 6, 1278 (1964).
4. A. E. Voitenko, "Acceleration of gas during compression in conditions of sharp-angle geometry," Zh. Prikl. Mekh. Tekh. Fiz., No. 4, 112-116 (1966).
5. B. K. Crowley and H. D. Glenn, in: Proc. Seventh Int. Shock Tube Symp. (I. I. Glass, editor), Toronto University Press, Toronto (1970), pp. 314-342.
6. K. P. Stanyukovich (editor), The Physics of Explosions [in Russian], Nauka, Moscow (1975).
7. L. N. Busurina, V. Ya. Gol'din, N. N. Kalitkin, and L. S. Tsareva, "Numerical calculation of detonations," Zh. Vychisl. Mat. Mat. Fiz., 10, 239 (1970).
8. Ya. B. Zel'dovich and Yu. P. Raizer, Physics of Shock Waves and High-Temperature Gasdynamic Phenomena [in Russian], Nauka, Moscow (1963).
9. S. I. Anisimov, Ya. A. Imas, G. S. Romanov, and Yu. V. Khodyko, The Action of High-Power Radiation on Metals [in Russian], Nauka, Moscow (1963).
10. N. N. Kalitkin and L. V. Kuz'mina, "Tables of quantum-statistical equations of state of eleven elements," Manuscript deposited in the All-Union Institute of Scientific and Technical Information No. 2192-75, Moscow (1975).
11. B. K. Crowley, "PUFL, an 'almost-Lagrangian' gasdynamic calculation for pipe flows with mass entrainment," J. Comput. Phys., 2, 61 (1967).
12. V. F. Kuropatenko, "Equation of state of the detonation products of condensed charge of explosives," ChMMSS Novosibirsk, 8, No. 6, 68 (1977).
13. N. M. Kuznetsov, Thermodynamic Functions and Shock Adiabatic Curves of Air at High Temperature [in Russian], Mashinostroenie, Moscow (1965).
14. M. A. El'yashevich, F. N. Borovik, S. I. Kas'kova et al., Proc. Sixth All-Union Conf. on the Dynamics of Radiating Gas [in Russian], Moscow (1980), pp. 16-17.
15. N. N. Kalitkin and L. V. Kuz'mina, "Quantum-statistical equation of state of mixtures of elements," Manuscript deposited in the All-Union Institute of Scientific and Technical Information, No. 1128-76, Moscow (1976).
16. I. V. Avilova, L. M. Biberman, V. S. Vorob'ev, et al., Optical Properties of Hot Air [in Russian], Nauka, Moscow (1970).
17. D. R. Sawle, "Characteristics of the Voitenko high-explosive-driven gas compressor," Astronaut. Acta, 14, 393 (1969).

18. A. E. Voitenko and V. I. Kirko, "The efficiency of explosion plasma compressor," Fiz. Goreniya Vzryva, No. 6, 956-958 (1975).

UNIDIRECTIONAL NONSTATIONARY FLOW OF INSTANTANEOUSLY HEATED GAS FROM A CYLINDER FOR DIFFERENT POSITIONS OF THE HEATED ZONE

E. T. Bruk-Levinson, O. G. Martynenko, and E. A. Romashko

UDC 533.17.536.414

The finite-difference method and one-dimensional approximation are used to consider the processes of decay of an initial pressure discontinuity for the individual cases of its position in a bounded region.

The classical problem of one-sided and two-sided nonstationary flows of gas from a cylinder as a result of an increased initial pressure in the cylinder is encountered in various modifications in the study of gasdynamic processes in many technical devices, e.g., in shock tubes.

One encounters physical situations in which the residual pressure in the cylinder is created by instantaneous heating of the gas. The development of the nonstationary process depends here, in particular, on the relationship between the lengths of the cylinder and of the heated zone, and also on the position of this zone.

In the present work we numerically study the decay of a pressure discontinuity in a cylinder of finite length. One end of the cylinder is open to the atmosphere at finite pressure and the other end is insulated at various positions of the heated zone, which can take up the whole volume, or part of the volume near the open end, near the closed end, or in the center of the cylinder.

The problem was solved in the one-dimensional approximation, and the processes were assumed to be adiabatic. However, instead of the adiabatic curve, we used the general equation of state. This is because, in the thermodynamic viewpoint, the system in question is not closed, i.e., the parameters of the gas flowing into the system from the external medium at the suction stage do not satisfy the equation of the adiabatic curve for the initial working substance. In the equation of motion we took into account the force of viscous friction averaged over the cross section. The local resistance at the open end was taken into account in the form of a boundary condition — as a pressure drop proportional to the square of the outflow velocity. The initial distributions of pressure and temperature were determined by the position of the heated zone. The system of equations that describes the nonstationary process has the form

$$\begin{gathered}\frac{\partial u}{\partial t}+u\frac{\partial u}{\partial x}=-\frac{1}{\rho}\frac{\partial p}{\partial x}-\frac{\tau_0\chi}{\rho F},\\ \frac{\partial \rho}{\partial t}+\frac{\partial}{\partial x}(\rho u)=0,\\ \frac{\partial T}{\partial t}+u\frac{\partial T}{\partial x}+(k-1)T\frac{\partial u}{\partial x}=0,\\ p/\rho T=\text{const},\ \text{const}=p_1/\rho_0 T_1.\end{gathered}\tag{1}$$

Here T_1, p_1, ρ_0 are the initial values of temperature, pressure, and density of the gas, respectively.

A. V. Lykov Institute of Heat and Mass transfer. Academy of Sciences of the Belorussian SSR, Minsk. Translated from Inzhenerno-Fizicheskii Zhurnal, Vol. 43, No. 6, pp. 1020-1027, December, 1982. Original article submitted January 25, 1982.

0022-0841/82/4306-1425$07.50